Electron Population Analysis by Full-Potential X-Ray Absorption Simulations

Yves Joly,[1] Delphine Cabaret,[2,3] Hubert Renevier,[1] and Calogero R. Natoli[2]
[1]*Laboratoire de Cristallographie, CNRS, associé à l'Université Joseph Fourier, B.P. 166, F-38042 Grenoble Cedex 9, France*
[2]*Laboratori Nazionali di Frascati, INFN, Casella Postale 13, I-00044 Frascati, Italy*
[3]*Laboratoire de Minéralogie-Cristallographie, UPMC/UDD, Tour 16, Case 115, 4 Place Jussieu, F-75252 Paris Cedex 05, France*
(Received 27 July 1998)

We present the first successful attempt at calculating cluster full-potential x-ray absorption near-edge structure (XANES) spectra, based on the finite difference method. By fitting XANES simulations onto experimental spectra we are able to perform electron population analysis. The method is tested in the case of Ti K-edge absorption spectrum in TiO_2, where the amount of charge transfer between Ti and O atoms and of the screening charge on the photoabsorber is obtained taking into account both dipolar and quadrupolar transitions. [S0031-9007(99)08724-4]

PACS numbers: 78.70.Dm, 02.70.Bf, 71.20.Ps

The close interplay between experimental measurements and theoretical analysis has been and continues to be one of the most fruitful approaches to our present understanding of the electronic structure of condensed matter. This has become particularly true following the advent of synchrotron radiation experiments with their highly sophisticated detection techniques, since they provide a wealth of information impossible to exploit completely without the assistance of an adequate theoretical analysis.

The study of the occupied and unoccupied electronic states of matter by x-ray emission and absorption is one such instance. Traditionally band structure calculations in periodic systems have been of great help in this interaction process, especially for the occupied part of the states or the unoccupied part very near to the Fermi energy (10–15 eV). Nowadays one can perform very sophisticated full-potential self-consistent band calculations that can be used to advantage to analyze experimental data. However there are severe limitations regarding their applicability to systems of physical interest: (a) They can be applied only to periodic crystals; (b) band programs are not geared for calculating empty states far above the Fermi level (apart from an early attempt [1] that has remained isolated); (c) the charge relaxation around the core hole is difficult to implement (supercell calculations have to be done but it is not at all easy to reach self-consistency).

In this respect short range cluster calculations [2] are far more flexible and superior, since they can be applied to the vast majority of interesting cases (in material science, e.g., nanostructured materials, biology and coordination chemistry, catalysis and industrial processes, disordered systems, absorbates, etc.), and the energy range over which absorption spectra can be calculated is virtually unlimited. Incidentally even for periodic systems a long range band calculation is not necessary, for the simple physical reason that the finite lifetime of the excited photoelectron in the final state limits the size of the region sampled around the photoabsorber.

Unfortunately up to now cluster calculations have been based on multiple scattering theory with optical potential restricted to the muffin-tin approximation. This is a very limiting feature, especially at low photoelectron kinetic energies [the x-ray absorption near-edge structure (XANES) part of an absorption spectrum within about 50 eV from the edge], since then the excited electron becomes rather sensitive to the spacial and electronic details of the potential. The ability to perform full-potential cluster calculations would provide a unique way for utilizing the near-edge absorption region, not only for extracting structural geometrical information but also, in a novel way as illustrated below, to study the details of the effective potential and the distribution of charge density.

The purpose of the present paper is to present a viable method for doing such calculations and to apply it to the case of TiO_2-rutile, where full potential band calculations are possible for comparison, presenting at the same time a population analysis based on the novel way of using a XANES spectrum.

In the one-electron quadrupolar approximation the photoabsorption cross section with light polarized along the vector $\boldsymbol{\varepsilon}$, using Rydbergs and atomic units, is given by

$$\sigma = 4\pi^2 \alpha E_\nu \sum_f \Big(|\langle \overline{\Psi}^f | \boldsymbol{\varepsilon} \cdot \mathbf{r} | \Psi^i \rangle|^2 + \frac{1}{4} |\langle \overline{\Psi}^f | \boldsymbol{\varepsilon} \cdot \mathbf{r}\, \mathbf{k} \cdot \mathbf{r} | \Psi^i \rangle|^2 \Big), \quad (1)$$

where α is the fine structure constant, E_ν and $\mathbf{k}$ the photon energy and wave vector. Ψ^i and $\overline{\Psi}^f$ stand for the wave functions of the initial and final states. These latter are time-reversed scattering solutions of the Schrödinger equation (SE) [3]. With Ψ^i being known for core absorption, the problem is calculating all the possible final states.

In an *ab initio* cluster approach this is accomplished by solving the SE for the photoelectron moving in an effective optical potential of the Hedin-Lundqvist type [4],

 0031-9007/99/82(11)/2398(4)$15.00

using the finite difference method (FDM) full potential approach [5].

The FDM has been known for a long time [6] but it is only recently that the first FDM band structure calculation was reported [7]. The technique was also extended to low energy electron [8] and positron diffraction [9]. Sensitivity of low energy particles on electronic parameters was illustrated in Ref. [10]. The calculation is performed on a sufficiently large cluster around the central atom. Following Dill and Dehmer [11], the whole space is divided in three regions: (i) an outer sphere region surrounding the cluster of interest, (ii) an atomic region composed by very little spheres (up to 0.65 Å of radius) around the atomic cores (not the usual large muffin-tin spheres), and (iii) the interatomic region where an FDM formulation of the Schrödinger equation is performed. In the outer sphere region, the potential is assumed constant and a complete set of scattering solutions is given by an expansion of the final states in spherical harmonics $L_f = (\ell_f, m_f)$,

$$\Psi^f(\mathbf{r}) = \sqrt{\frac{\kappa}{\pi}}\left(j_{\ell_f}(\kappa r)Y_{L_f}(\hat{\mathbf{r}}) + \sum_L T_L^{L_f} h_\ell^+(\kappa r)Y_L(\hat{\mathbf{r}})\right),$$

where j_l and h_l^+ are the radial Bessel and outgoing Hankel functions. $\kappa = \sqrt{E}$ is the electronic wave vector and E is the kinetic energy of the photoelectron in the outer sphere. The quantities $T_L^{L_f}$ are the unknown cluster scattering amplitudes to be determined in the way specified below. The factor κ/π assures normalization of the scattering wave function to one state per Rydberg. In the atomic core region, since the potential is spherically symmetric to a very good approximation, one can expand the solution as

$$\Psi^f(\mathbf{r}) = \sum_L A_L^{L_f} R_\ell(r)Y_L(\hat{\mathbf{r}}),$$

where the functions $R_\ell(r)$ are solutions of the radial SE inside the atoms, with the vector $\mathbf{r}$ being measured from the atomic centers.

Finally in the interatomic region, the unknowns are the values of the wave function on each grid point i: $\Psi_i^f = \Psi^f(\mathbf{r}_i)$. Here the Laplacian is discretized by approximating the wave function around the point i by a polynomial of the order of 4. In this way, in an orthogonal frame, the SE becomes

$$[6 + h^2(V_i - E)]\Psi_i^f - \frac{16}{15}\sum_j^{\text{first}} \Psi_j^f + \frac{1}{15}\sum_j^{\text{second}} \Psi_j^f = 0,$$

where h is the interpoint distance (the smaller it is, the more accurate is the computation). In the XANES energy range, convergence is reached with h around 0.25 Å. $V_i = V(\mathbf{r}_i)$ is the potential on the node point i. The summations are, respectively, over the six first and the six second neighbor points in the three orthogonal directions. The resulting large system of linear equations connecting the values of the wave function on all the grid points in the interstitial region and the expansion amplitudes $A_L^{L_f}$ and $T_L^{L_f}$ within the atomic core region and the outer sphere, respectively (in a way dictated by the continuity of the wave function and its gradient across the surface boundaries between the different regions), is solved by the Gauss-Seidel method to provide the solution everywhere in space. Equation (1) provides then the absorption coefficient.

This formulation does not require any approximation on the shape of the optical potential. This latter, moreover, to a very good approximation, can be assumed to be a functional of the total electronic density relaxed about the core hole. Therefore the shape of a XANES spectrum is determined not only by the position of the atoms around the photoabsorber (which convey structural information), but also, although to a lesser extent, by the electronic density of the system. This fact suggests a novel way of exploiting near-edge XAS spectra.

Indeed the total electronic density can be described by the superposition of the charge densities of the atoms whether neutral or ionized according to the system. A key ingredient in this procedure is the type of atomic orbitals, since this latter is correlated to the electron population. In particular, bond directed valence orbitals are used whenever appropriate. For neutral or positively charged atoms, we take the orbitals generated via an atomic relativistic Hartree-Fock (HF) calculation. For anions we use the same HF program but dilate the resulting orbitals. This dilatation is controlled by the radius of the orbital defined at the maximum of the radial electron density. The electron population and the anion orbital radius are adjusted by minimizing the discrepancy between the simulated and the experimental spectrum. In order to have an optimization criterium we use the reliability factor of type D_1 as described in Ref. [12] to measure the "distance" between the two curves.

We have chosen to illustrate our method with an application to the polarized Ti K-edge x-ray absorption spectra in the rutile TiO_2 structure for a variety of reasons. First, being a closed shell system, no multiplet effects are expected in the final state. Multielectron excitations (of the type $3p$ to $4p$ at around 30 eV above the rising edge) are not observed, being probably very weak. Therefore we can reasonably expect a one-electron approach to be accurate enough for the study of charge-transfer transitions. Both dipole and quadrupole transitions are allowed [Eq. (1)]. Calculated polarized spectra are compared with the experiments of Poumellec *et al.* [13] for two different directions of the electric field and of the propagation vector: (a) $(\boldsymbol{\varepsilon}, \mathbf{k}) = ([001], [110])$, and (b) $(\boldsymbol{\varepsilon}, \mathbf{k}) = ([1\bar{1}0], [110])$. We use basis vectors rotated by 45° around the z axis of the conventional crystallographic structure to get the mirror planes along xOy, xOz, and yOz. In the structure, there are two kinds of octahedra related to each other by a rotation of 90° around the z axis. The symmetry type of the orbitals reached in the final state in the various experimental setups are (a) p_z for the dipolar transition and d_{xz} and d_{yz} for the quadrupolar transitions; (b) p_x

and p_y for the dipolar but only d_{xy} for the quadrupolar. According to the ligand field theory applied in our frame, the d_{xy} and d_{yz} orbitals belong to the t_{2g}-like representation; d_{xz} belongs to the e_g-like representation. The final result of the fitting is shown in Fig. 1, where the experimental (dotted line) and theoretical spectra (solid line) are superimposed for the two experimental setups (a) (top) and (b) (bottom). Cluster size convergence was reached with a radius of 6.9 Å. The agreement between experiment and theory is very good: all the features are well reproduced both in amplitude and position and in both orientations. Since the correct interpretation of the three peaks (A_1, A_2, and A_3) is still controversial, the pre-edge region in both polarizations is detailed in Fig. 2. There the individual quadrupolar and dipolar components are also plotted. One can observe that A_2 and A_3 are higher when $\boldsymbol{\varepsilon}$ is along the c axis than when it is perpendicular to it. On the contrary, A_1 is lower in the first polarization. One can see that the shape of the A_2 peak is also well reproduced, its width being larger in the second orientation. The quadrupolar contribution is significant: the A_1 peak is only quadrupolar t_{2g}; A_2 is dipolar in nature but includes also a little e_g quadrupolar component; A_3 is a pure dipolar feature. All of this is in agreement with Uozumi *et al.* [14] but not with Wu *et al.* [15] and Brydson *et al.* [16] who, relying on muffin-tin calculations, attribute the A_1 feature to a dipolar transition. Clearly on the basis of the present findings, this is an artifact of the muffin-tin approximation.

As already mentioned, our interest is not only the full potential cluster calculation of XANES but also the evaluation of the electronic parameters via the fitting procedure. In the present case the adjustable parameters were the Ti-3d orbital occupation numbers: n_d^* for the photoabsorber and n_d for the others titanium. n_d^* includes the amount of screening charge on the central atom. The O-2p orbital n_p is given by charge neutrality ($n_p = 6 - n_d/2$). No occupation of 4s orbital on Ti was present. The fitting procedure gives $n_d^* = 1.91$, $n_d = 1.00$, and $n_p = 5.50$. The quadrupolar transition is extremely sensitive to the n_d^* parameter, contrary to the dipolar transition, as already emphasized in Ref. [14]. Thus it is the fit of the energy position of peak A_1 that allows the evaluation of n_d^* with high accuracy. A calculation with $n_d = 2.00$ showed that the quadrupolar transition A_1 shifted upward in energy by 2.0 eV, hence with a slope of 2.0 eV per 0.1 electron of screening charge. The fact that the core hole charge is not completely screened (0.1 electron charge is missing), points to a correlation effect caused by the presence of the excited 3d electron that hinders the screening process. The interesting comparison with the same quantity for the dipolar transition cannot be done, due to the already mentioned poor sensitivity of the spectral shape to the screening charge. n_d was optimized especially with peaks A_2 and A_3 in the experimental spectra, judging from their energy distance from feature D in Fig. 1. Their energy position was quite sensitive to the amount of charge transfer between Ti and O atoms with a derivative of 0.6 eV per tenth of electron on titanium. This allowed a precise evaluation of the occupation numbers. Also their amplitude variation with polarization did agree with the data as shown in Fig. 2. However this parameter does not affect only the A_2 and A_3 peaks but also all the spectral shapes up to feature C. The minimization of the R factor (inset

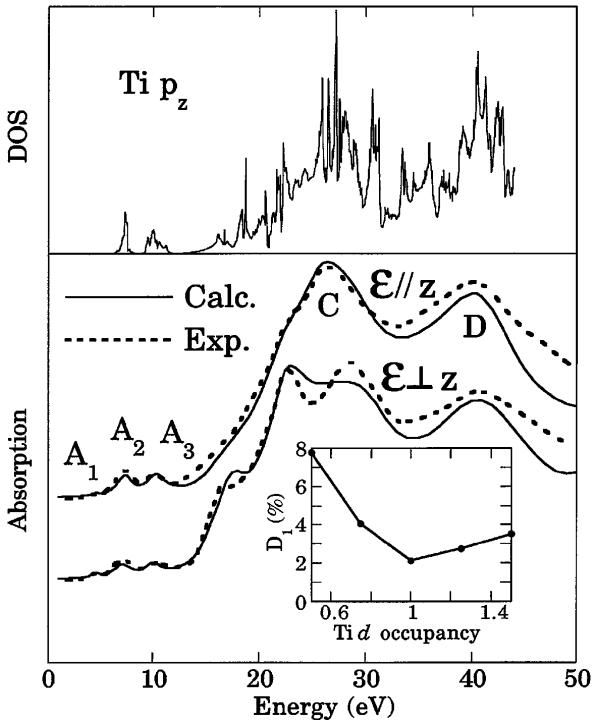

FIG. 1. Lower panel: Comparison between the experimental (dotted line) and calculated (solid line) Ti K-edge XANES spectra of single crystal TiO_2-rutile for two orientations of the electric field and wave vectors; bottom: $(\boldsymbol{\varepsilon}, \mathbf{k}) = ([1\bar{1}0], [110])$ $(\boldsymbol{\varepsilon} \perp \mathbf{k})$ top: $(\boldsymbol{\varepsilon}, \mathbf{k}) = ([001], [110])$ $(\boldsymbol{\varepsilon} \parallel \mathbf{k})$. Inset: Variation of the R factor with the Ti 3d occupancy. Upper panel: p_z-projected density of states on Ti atom calculated by the FLAPW method.

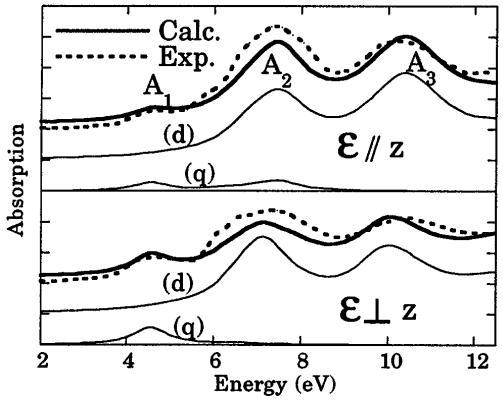

FIG. 2. View of the pre-edge region. Quadrupolar (q) and dipolar (d) components and their sum for $\boldsymbol{\varepsilon} \parallel$ (top) and $\perp$ (bottom) to z. The dotted line is the experimental curve.

of Fig. 1) which is carried out on the considered energy region confirms our results.

For comparison band structure calculations were performed within the full-potential linearized augmented plane wave (FLAPW) framework of Ref. [17], obtaining agreement with similar calculations by Sorantin and Schwarz [18]. The p_z-projected density of states on the Ti atom is also shown in Fig. 1 and confirms the assignment of the pre-edge features, since only two peaks are found just above the Fermi level at the same energy position as the Ti $3d$ projected density of states. Straight comparison with the orbital occupation number cannot be done, but we can get an idea about the distribution of the valence charge by integrating the total charge inside two equal nonoverlapping spheres around Ti and O atoms with a radius of 0.95 Å. We get, respectively, 18.88 and 7.80 electrons with the FLAPW method, 18.85 and 8.17 with our approach, the rest of the charge being in the interstitial region. The agreement is very good for Ti and seems less good for O. The discrepancy might be significant and could indicate a tendency to localization of the O electrons due to correlation effects. In any case the 0.95 Å radius used for the integration and corresponding to the sphere where the expansion in spherical waves is performed in the FLAPW method (see Appendix of [18]) does not correspond to the ionic radius of the atom. On the other hand, recalculating the absorption spectrum using the self-consistent density generated by FLAPW resulted in a R factor slightly higher than our minimum ($D_1 = 2.53\%$ to be compared with the $D_1^{\min} = 2.14\%$). Moreover that calculation cannot yield any information about the core hole screening charge and is unable to reproduce the A_1 feature.

Another interesting comparison is with the valence-band structure of TiO_2 performed by Hardman *et al.* [19]. They use an *ab initio* atomic orbital-based method and find a converged $3d$ orbital occupancy of 1.65 electrons for Ti atoms. This result is quite at a variance both with our calculations and FLAPW calculations. However the self-consistent procedure in Ref. [19] was carried out "only to the extent that the energy of the Ti d state was made consistent with that in a neutral atom with the same d-orbital occupancy." The FLAPW method instead uses the framework of the density functional theory, where the total energy of the system is minimized. Therefore it should provide more reliable results concerning the total charge density.

A further comparison can be done with the work of Uozumi *et al.* [14]. By studying the pre-edge structure of TiO_2, these authors adopt a $Ti_{11}O_6$ cluster to describe the system with a Hamiltonian of the impurity-Anderson-like form with Coulomb, crystal field and overlap integrals parameters estimated on the basis of band calculations and HF terms suitably reduced. They come up with an estimated $n_d = 0.8$. In another study Okada and Kotani [20] analyze the Ti $2p$ x-ray photoemission and absorption spectra in TiO_2 by means of a TiO_6 model, using the same type of Hamiltonian. From a comparison with experiments they deduce a ground state consisting of $|3d^0\rangle$, $|3d^1\underline{L}\rangle$, and $|3d^2\underline{L}^2\rangle$ states, in the respective proportion of $\alpha_0 = 39.5\%$, $\alpha_1 = 48.2\%$, and $\alpha_2 = 12.3\%$, resulting in an average $3d$ occupation number of 0.73 electrons. There is a tendency in these calculations to overestimate the intra-atomic correlations and one may notice that the calculated n_d increases with the size of the model cluster. In any case their values are not totally incompatible with our findings.

Summarizing, we have tried to give convincing evidence that XANES spectra can be used to do an electron population analysis at least in those cases where the excitation process can be reasonably well described in terms of one electron moving in an effective optical potential of the local-density type. Many interesting systems fall under this category. For example, the present procedure could be easily extended to the analysis of spin-up and spin-down charge densities in magnetic materials using dichroic spectra or to the study of the validity of the final state rule by monitoring the charge relaxation around the core hole.

We thank Ch. Brouder for fruitful discussions.

[1] J. E. Müller and J. W. Wilkins, Phys. Rev. B **29**, 4331 (1984).
[2] C. R. Natoli, D. K. Misemer, S. Doniach, and F. W. Kutzler, Phys. Rev. A **22**, 1104 (1980); P. J. Durham, J. B. Pendry, and C. H. Hodges, Solid State Commun. **38**, 159 (1983).
[3] G. Breit and H. A. Bethe, Phys. Rev. **93**, 888 (1954).
[4] L. Hedin and S. Lundqvist, Solid State Phys. **23**, 1 (1969).
[5] Y. Joly, in *Proceedings of the XAFS IX Conference* [J. Phys. IV (France) **7**, C2-111 (1997)].
[6] G. E. Kimball and G. H. Shortley, Phys. Rev. **45**, 815 (1934).
[7] J. M. Thijssen and J. E. Inglesfield, Europhys. Lett. **27**, 65 (1994).
[8] Y. Joly, Phys. Rev. Lett. **68**, 950 (1992).
[9] Y. Joly, Phys. Rev. Lett. **72**, 392 (1994).
[10] Y. Joly, Phys. Rev. B **53**, 13 029 (1996).
[11] D. Dill and J. L. Dehmer, J. Chem. Phys. **61**, 692 (1974).
[12] J. Philip and J. Rundgren, in *Proceedings of the Conference on Determination of Surface Structure by LEED, Yorktown Heights, 1980,* edited by P. M. Marcus (Plenum, New York, 1984).
[13] B. Poumellec *et al.,* Phys. Status Solidi (b) **164**, 319 (1991).
[14] T. Uozumi *et al.,* Europhys. Lett. **18**, 85 (1992).
[15] Z. Y. Wu *et al.,* Phys. Rev. B **55**, 10 382 (1997).
[16] Brydson *et al.,* J. Phys. Condens. Matter **1**, 797 (1989).
[17] P. Blaha, K. Schwartz, and P. I. Sorantin, Comput. Phys. Commun. **59**, 399 (1990).
[18] P. I. Sorantin and K. Schwarz, Inorg. Chem. **31**, 567 (1992).
[19] P. J. Hardman *et al.,* Phys. Rev. B **49**, 7170 (1994).
[20] K. Okada and A. Kotani, J. Electron Spectrosc. Relat. Phenom. **62**, 131 (1993).